International Geology Review, 2013
Vol. 55, No. 7, 904–916, http://dx.doi.org/10.1080/00206814.2013.767496

Taylor & Francis
Taylor & Francis Group

Geological and C–O–S–Pb–Sr isotopic constraints on the origin of the Qingshan carbonate-hosted Pb–Zn deposit, Southwest China

Jia-Xi Zhou[a]*, Zhi-Long Huang[a], Jian-Guo Gao[b] and Zai-Fei Yan[a]

[a]*State Key Laboratory of Ore Deposit Geochemistry, Institute of Geochemistry, Chinese Academy of Sciences, Guiyang 550002, China;*
[b]*Faculty of Land Resource Engineering, Kunming University of Science and Technology, Kunming 650093, China*

(*Accepted 6 January 2013*)

Located in the western Yangtze Block, the Qingshan Pb–Zn deposit, part of the Sichuan–Yunnan–Guizhou Pb–Zn metallogenic province, contains 0.3 million tonnes of 9.86 wt.% Pb and 22.27 wt.% Zn. Ore bodies are hosted in Carboniferous and Permian carbonate rocks, structurally controlled by the Weining–Shuicheng anticline and its intraformational faults. Ores composed of sphalerite, galena, pyrite, dolomite, and calcite occur as massive, brecciated, veinlets, and disseminations in dolomitic limestones.

The C–O isotope compositions of hydrothermal calcite and S–Pb–Sr isotope compositions of Qingshan sulphide minerals were analysed in order to trace the sources of reduced sulphur and metals for the Pb–Zn deposit. $\delta^{13}C_{PDB}$ and $\delta^{18}O_{SMOW}$ values of calcite range from –5.0‰ to –3.4‰ and +18.9‰ to +19.6‰, respectively, and fall in the field between mantle and marine carbonate rocks. They display a negative correlation, suggesting that CO_2 in the hydrothermal fluid had a mixed origin of mantle, marine carbonate rocks, and sedimentary organic matter. $\delta^{34}S$ values of sulphide minerals range from +10.7‰ to +19.6‰, similar to Devonian-to-Permian seawater sulphate (+20‰ to +35‰) and evaporite rocks (+23‰ to +28‰) in Carboniferous-to-Permian strata, suggesting that the reduced sulphur in hydrothermal fluids was derived from host-strata evaporites. Ores and sulphide minerals have homogeneous and low radiogenic Pb isotope compositions ($^{206}Pb/^{204}Pb$ = 18.561 to 18.768, $^{207}Pb/^{204}Pb$ = 15.701 to 15.920, and $^{208}Pb/^{204}Pb$ = 38.831 to 39.641) that plot in the upper crust Pb evolution curve, and are similar to those of Devonian-to-Permian carbonate rocks. Pb isotope compositions suggest derivation of Pb metal from the host rocks. $^{87}Sr/^{86}Sr$ ratios of sphalerite range from 0.7107 to 0.7136 and $(^{87}Sr/^{86}Sr)_{200Ma}$ ratios range from 0.7099 to 0.7126, higher than Sinian-to-Permian sedimentary rocks and Permian Emeishan flood basalts, but lower than Proterozoic basement rocks. This indicates that the ore strontium has a mixture source of the older basement rocks and the younger cover sequence. C–O–S–Pb–Sr isotope compositions of the Qingshan Pb–Zn deposit indicate a mixed origin of the ore-forming fluids and metals.

Keywords: C–O–S–Pb–Sr isotopes; sources of ore-forming fluids and metals; Qingshan carbonate-hosted Pb–Zn deposit; Southwest China

1. Introduction

More than 400 Pb–Zn–Ag–Ge deposits have been reported in the western Yangtze Blocks, Southwest China (Figure 1A). They form the important Sichuan–Yunnan–Guizhou (SYG) Pb–Zn metallogenic province, contain total Pb and Zn metals of more than 20 million tonnes (Mt) at grades of >10% Pb + Zn, and have been the major source of base metals in China (Cromie *et al.* 1996; Liu and Lin 1999). However, the origin of these deposits and the mechanism for such giant accumulations of Pb–Zn–Ag–Ge have long been controversial (e.g. Xie 1963; Liao 1984; Tu 1984; Chen 1986; Zheng and Wang 1991; Liu and Lin 1999; Deng *et al.* 2000; Zhou *et al.* 2001, 2010, 2011, 2013; Huang *et al.* 2003, 2010; Han *et al.* 2004, 2007, 2012; Hu and Zhou 2012).

The Pb–Zn deposits in the SYG province are hosted in Sinian (late Proterozoic) to late Permian carbonate rocks (e.g. Zheng and Wang 1991; Zhou *et al.* 2001, 2011; Han *et al.* 2007, 2012). A close association of these deposits with the Permian Emeishan flood basalts led Xie (1963) to classify them as distal magmatic-hydrothermal deposits. On the other hand, Tu (1984) interpreted them as strata-bound ore deposits and proposed that they were generated during hydrothermal reworking of sedimentary rocks. This view was popular in the 1980s and 1990s (e.g. Liao 1984; Chen 1986; Wang 1993). Some Pb–Zn deposits in the SYG province were later re-interpreted to be typical Mississippi valley-type deposits (e.g. Zheng and Wang 1991; Wang *et al.* 2000, 2003, 2010; Zhou *et al.* 2001; Leach *et al.* 2010). The Permian Emeishan flood basalts have also been

*Corresponding author. Email: zhoujiaxi@vip.gyig.ac.cn

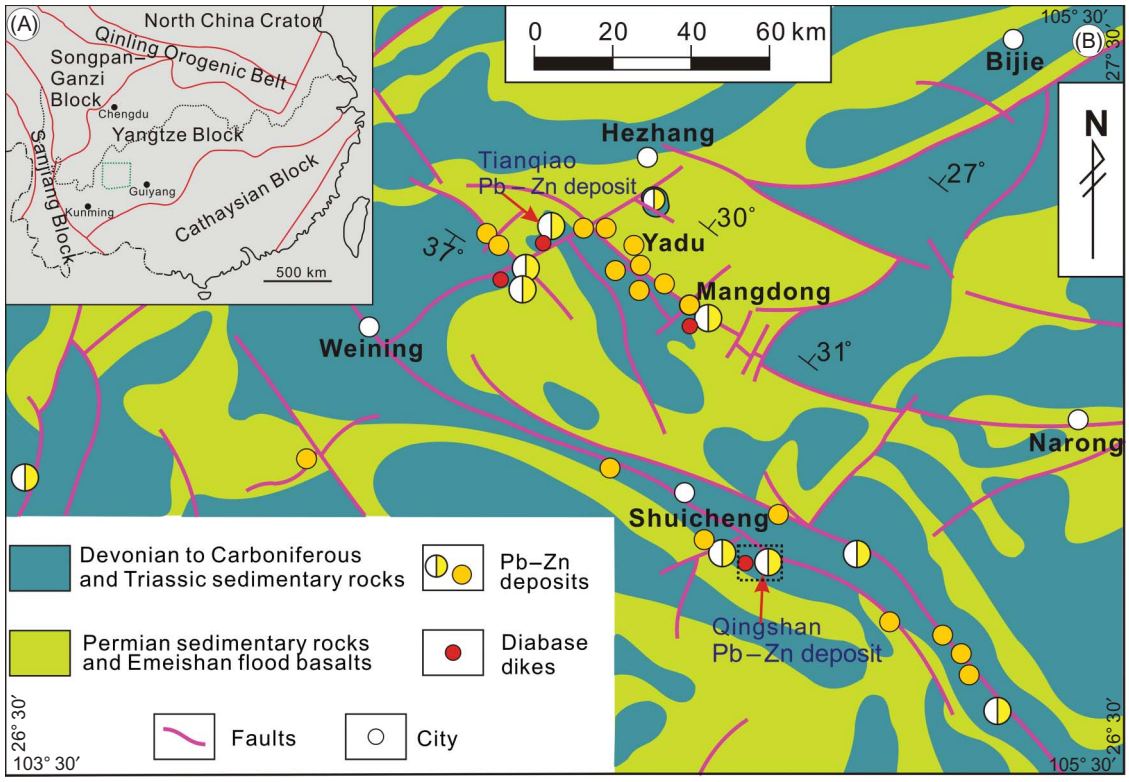

Figure 1. (A) Regional geological setting and (B) sketch geological map of NW Guizhou Pb–Zn metallogenic province.

considered to be an important source of ore-forming metals and heat (e.g. Liu and Lin 1999; Huang *et al.* 2003, 2004, 2010; Han *et al.* 2004, 2007, 2012). However, despite many investigations and the large number of publications in Chinese, it is still unclear how these metals became so highly concentrated in the SYG province.

In the southeastern SYG province, more than one hundred Pb–Zn deposits have been reported, most of which are distributed along the NW-trending Weining–Shuicheng and Yadu–Mangdong faults (Figure 1B). Previous studies are only available in the Chinese literature but have documented that all these deposits occur in Devonian to Permian dolomitic limestone (e.g. Chen 1986; Wang 1993; Zheng 1994; Gu *et al.* 1997; Mao *et al.* 1998; Zhang *et al.* 1999; Fu 2004; Gu 2007; Jin 2008; Zhou *et al.* 2011). The Qingshan Pb–Zn deposit along the Weining–Shuicheng fault (Figure 1B) has been mined over the past decade (Jin 2008). Gu *et al.* (1997) and Zhang *et al.* (1999) examined its geology and considered it to be a sediment-reworked deposit.

C–O–S–Pb–Sr isotopes are powerful tools for determining sources of ore-forming fluids and metals (e.g. Zheng and Wang 1991; Huston *et al.* 1995; Ohmoto and Goldhaber 1997; Zhou *et al.* 2001, 2010, 2013; Wilkinson *et al.* 2005; Han *et al.* 2007; Huang *et al.* 2010; Yavuz *et al.* 2011; Dou and Zhou 2013). Multiple isotopic studies of the Qingshan Pb–Zn deposit are not available, but may provide important insights into its genesis. In this article, we describe the geology of the Qingshan Pb–Zn deposit and report a new C–O isotope for hydrothermal calcite and a S–Pb–Sr isotope for sulphide minerals. These new datasets, together with previously published results are utilized to constrain the sources of ore-forming fluids and metals. We discuss the implications of our study for the giant Pb–Zn accumulation in the SYG province.

2. Geological background

2.1. Regional geology

In the western Yangtze Block, the sedimentary sequences include the ~1.7 Ga Dongchuan and ~1.1 Ga Kunyang Groups and equivalents, which represent the folded basement (Sun *et al.* 2009; Zhao *et al.* 2010). They are unconformably overlain by Palaeozoic and lower Mesozoic strata of shallow marine origin (Yan *et al.* 2003). Jurassic to Cenozoic strata are entirely continental facies (Liu and Lin 1999). A major feature of the western Yangtze Block is the mantle plume-derived Emeishan Large Igneous Province, covering an area of more than 250,000 km^2 (Chung and Jahn 1995; Zhou *et al.* 2002). This igneous province is dominantly composed of volcanic rocks, known as Emeishan flood basalts (~260 Ma; Zhou *et al.* 2002), interlayered with Permian limestone.

2.2. Geology of the SYG metallogenic province

There have been about 408 Pb–Zn deposits reported in the western Yangtze Block, which distribute in a large triangular area of 170,000 km^2 in NE Yunnan, NW Guizhou, and SW Sichuan provinces (Liu and Lin 1999). They are characterized by irregular ore bodies with simple mineralogy, weak wall rock alteration, and high Pb + Zn grade ores (e.g. Zheng and Wang 1991; Zhou *et al.* 2001; Han *et al.* 2007), usually associated with Ag, Ge, Cd, Ga, and In (e.g. Han *et al.* 2007; Zhou *et al.* 2011) and hosted in dolomitic limestone or dolostone of Sinian to Permian (e.g. Liu and Lin 1999; Wang *et al.* 2000, 2003, 2010; Zhou *et al.* 2001, 2010, 2011, 2013; Jin 2008). Notably, the host strata are all below the lower Permian Emeishan flood basalts (e.g. Liu and Lin 1999; Huang *et al.* 2010).

2.3. Local geology

In the southeastern SYG province, the cover sequences include Devonian, Carboniferous, Permian, and Triassic sedimentary strata (Figure 1B), and Permian Emeishan flood basalts. Diabase dikes, locally present, may be part of the Emeishan Large Igneous Province and also occur in this region (Figures 1B and 2). The Devonian strata consist of sandstone, siltstone, limestone, and dolostone, and the Carboniferous strata are composed of shale, limestone, and dolostone. The early Permian sequence consists of sandstone, shale, coal layers, and limestone, all overlain by Permian Emeishan flood basalts. The basalts, in turn, are overlain by late Permian sandstone, siltstone, and coal measures. The Triassic strata consist of siltstone, sandstone, dolostone, and limestone. NW- and NE-striking faults are well developed and control the Pb–Zn deposits in this region.

3. Geology of the Qingshan deposit

The Qingshan Pb–Zn deposit is located on the middle part of the Weining–Shuicheng fault (Figure 1B). In the Qingshan mining field, the Carboniferous stratum is the Maping Formation, which chiefly consists of limestone and dolomitic limestone. The overlying lower Permian Liangshan Formation consists of shale, quartz sandstone, and argillaceous sandstone (Figure 2). Major ore bodies occur in dolomitic limestone of the Maping Formation and are structurally controlled by the Weining–Shuicheng anticline and its intraformational faults. The immediate host rocks of the ore bodies are dolomitic limestone in the upper part of the Maping Formation and shale in the lower part of the Liangshan Formation (Figure 2).

Underground mining and exploratory drilling provide excellent access to the three major ore bodies. No. 1 ore body is 145 m in depth, 70 m in length and 1.3–32 m in width. Ores in this body contain 0.2 Mt of Pb and Zn metals at grades of 9.92 wt.% Pb and 37.58 wt.% Zn. No. 2 ore body is 45 m in depth, 42 m in length, and 0.9–6.3 m in width and contains 0.06 Mt of Pb and Zn metals at grades of 9.22 wt.% Pb and 35.12 wt.% Zn. Ores in No. 3 ore body have grades of 3.76 wt.% Pb and 34.96 wt.% Zn. This ore body contains 0.03 Mt of Pb and Zn metals and is 40 m in depth, 30 m in length, and 0.5–3.6 m in width. Ores from the Qingshan deposit contain small amounts of Ge, Ga, Cd, and Ag (Gu *et al.* 1997). These trace metals are thought to be hosted in sphalerite and galena (Zhou *et al.* 2011). Ore bodies are strata bounded as tabular and lenticular bodies with sharp boundaries against the wall rocks (Figure 2). Some ore bodies contain galena, sphalerite, and pyrite veinlets hosted in dolomitic limestone. Banded ores consist of alternating layers rich in ore minerals or calcite.

Primary ores are massive, disseminated, or banded (Figure 3), and are composed of sphalerite, galena, and pyrite, with calcite and dolomite as gangue minerals. Ores from the Qingshan deposit have experienced diagenetic, hydrothermal, and oxidized periods. The hydrothermal period is composed of sulphide–carbonate and carbonate stages. There are two principal mineral assemblages formed in the sulphide–carbonate stage. In the pyrite–sphalerite–calcite assemblage (Figures 3C and 3D), sphalerite is fine- to coarse-grained (0.1–13 mm) with xenomorphic to automorphic granular textures. It is dark brown and occurs as massive, porphyritic, and banded forms or in disseminated aggregates. Individual grains are commonly skeletal but have well-developed cleavage. Pyrite is also coarse-grained (3–6 mm), has both octahedral and cubic forms, and commonly occurs as disseminations or bands in the wall rocks adjacent to the ores. Calcite is lumpy and patchy, about 9 cm in size. In the sphalerite–galena–calcite assemblage (Figures 3A and 3B), sphalerite is fine- to coarse-grained (0.06–11 mm) with xenomorphic to automorphic granular textures. It occurs in massive and banded forms or in disseminated aggregates and is brown-yellow in colour. Galena has a granular and corrugated texture. Individual grains are 0.2–14 mm in diameter, have cubic cleavage, and show obvious deformation. Calcite is patchy, about 5 cm in size.

Wall rock alterations include dolomitization, calcitization, Fe–Mn carbonatization, and ferritization, of which dolomitization and calcitization are closely associated with Pb–Zn mineralization. Fe–Mn carbonatization is a good indicator for ore prospecting, which is association with Pb–Zn mineralization. Ferritization is present mainly as veinlets and irregular nodules in dolostone or as gossan resultant from pyrite oxidization. Its distribution is not as extensive as dolomitization, but is closely associated with Pb–Zn mineralization. The intensity of ferritization is always correlated with that of Pb–Zn mineralization.

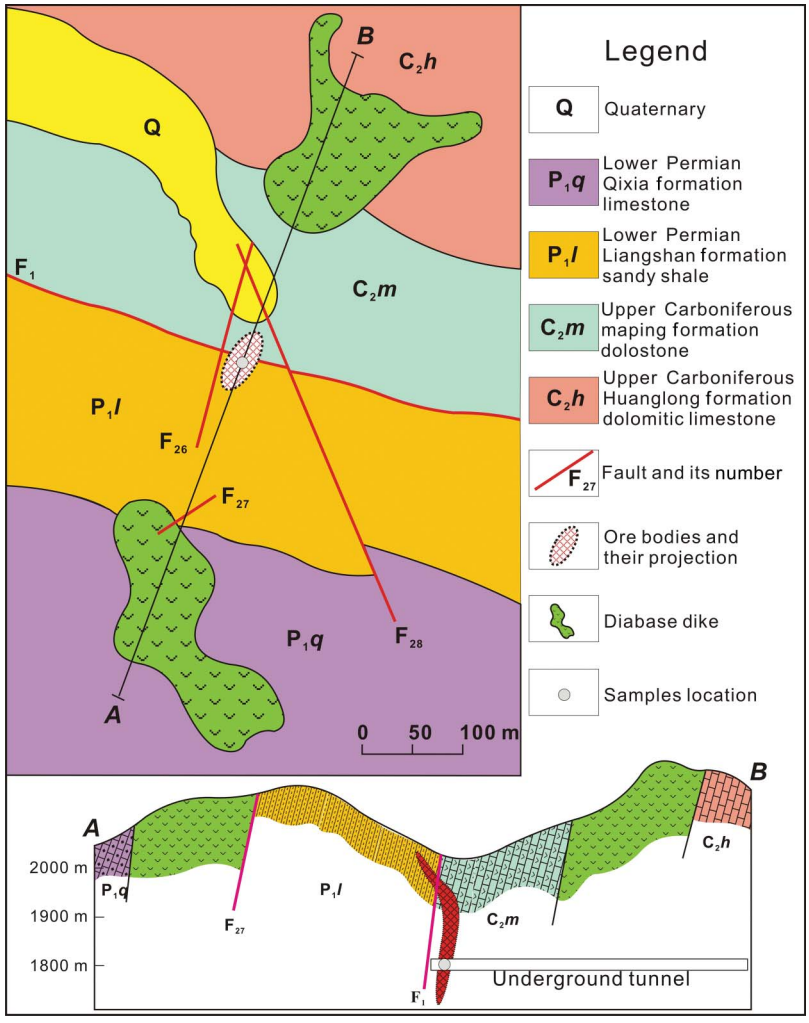

Figure 2. (A) Geological map of the Qingshan Pb–Zn deposit and (B) A–B geological profile.

4. Analytical methods

Ores from the Qingshan Pb–Zn deposit were crushed to 40–80 meshes, and pyrite, sphalerite, galena, and calcite were handpicked under a binocular microscope. Calcite was analysed for C–O isotope compositions and sulphide minerals for S–Pb–Sr isotope compositions.

C–O isotope compositions were obtained using a MAT–251 EM mass spectrometer at the State Key Laboratory of Environmental Geochemistry, Institute of Geochemistry, Chinese Academy of Sciences. Calcite reacts with pure phosphoric acid to produce CO_2. The analytical precisions (2σ) are ±0.2‰ for carbon isotopes and ±2‰ for oxygen isotopes. C–O isotope compositions are reported to PDB. $\delta^{18}O_{SMOW} = 1.03086 \times \delta^{18}O_{PDB} + 30.86$ (Friedman and O'Neil 1977).

S isotope analyses were carried out at the State Key Laboratory of Environmental Geochemistry, Institute of Geochemistry, Chinese Academy of Sciences, using a continuous flow mass spectrometer. GBW 04415 and GBW 04414 Ag_2S were used as the external standards, and the relative errors (2σ) were better than 0.1‰. Sulphur isotope compositions are reported to CDT.

Pb isotope analyses were carried out using the GV Isoprobe–T thermal ionization mass spectrometer at the Beijing Institute of Uranium Geology. The analytical procedure involved dissolution of samples using HF and $HClO_4$ in crucibles, followed by basic anion exchange resin to purify Pb. Analytical results for the standard NBS 981 are $^{208}Pb/^{204}Pb = 36.611 \pm 0.004$ (2σ), $^{207}Pb/^{204}Pb = 15.457 \pm 0.002$ (2σ), and $^{206}Pb/^{204}Pb = 16.937 \pm 0.002$ (2σ), in agreement with the reference value (Belshaw *et al.* 1998).

Chemical separation of Rb and Sr from matrix elements and mass spectrometric measurement were accomplished at the Institute of Geology and Geophysics, Chinese Academy of Sciences. A detailed analytical procedure for Rb–Sr isotope analyses is available in Li *et al.* (2005). Spec–Sr exchange resin of special efficiency was used for

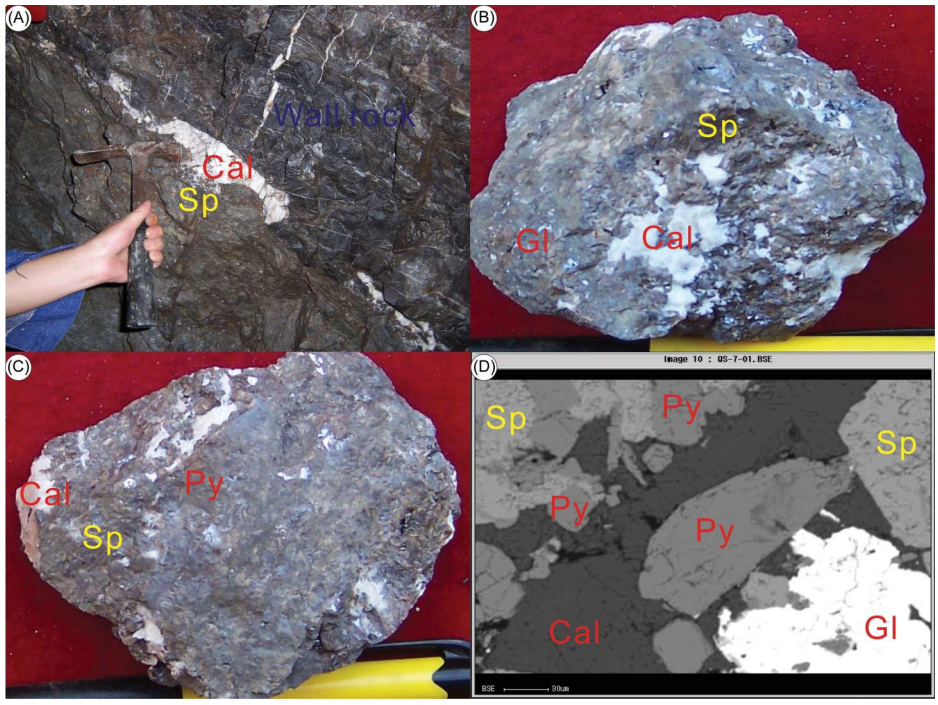

Figure 3. Minerals assemblages of the Qingshan Pb–Zn deposit. (A) Boundary of wall rocks and ore bodies; (B) sphalerite (Sp)–galena (Gl)–calcite (Cal) assemblage; (C) sphalerite–pyrite (Py) assemblage; and (D) Sphalerite–pyrite–galena–calcite assemblage.

the separation and purification of Rb and Sr. The whole procedural blank of both Rb and Sr was about 6 pg. Rb–Sr isotope compositions were measured by the Isoprobe–T thermal ionization mass spectrometer. An $^{88}Sr/^{86}Sr$ ratio of 8.37521 was used to calibrate mass fractionation of Sr isotope. The average $^{87}Sr/^{86}Sr$ ratio of NBS 987 was 0.710242 ± 5 (2σ, $n = 12$). The uncertainties (2σ) are 2% for $^{87}Rb/^{86}Sr$ ratios and 0.005% for Sr isotope compositions.

5. Analytical results

5.1. *Carbon and oxygen isotope compositions*

C and O isotope compositions of hydrothermal calcite and host carbonate rocks (Mao *et al.* 1998; Zhang *et al*. 1999) are listed in Table 1 and shown in Figure 4. Calcite has relatively uniform C and O isotope compositions with $\delta^{13}C_{PDB}$ values ranging from –5.0‰ to –3.4‰ and $\delta^{18}O_{SMOW}$ values ranging from +14.9‰ to +19.6‰. Limestone has

Table 1. C and O isotope compositions of hydrothermal calcite and limestone from the Qingshan Pb–Zn deposit.

Sample no.	Object	$\delta^{13}C_{PDB}$/‰	$\delta^{18}O_{SMOW}$/‰	Sources
Qs-w-04	Limestone	2.3	22.9	Mao *et al*. (1998)
Qs-w-05	Limestone	1.1	24.1	
QS-02	Limestone	1.8	24.3	
QS-03	Limestone	1.0	24.7	
HT-01	Limestone	0.6	24.4	Zhang *et al*. (1999)
HT-10	Limestone	0.9	23.8	
Qs-02	Limestone	1.7	23.4	
Qs-03	Limestone	1.0	23.9	
Qs-01	Limestone	2.3	23.3	
Qs-04	Limestone	1.1	22.1	
QS-09-01	Hydrothermal calcite	−3.6	19.2	This article
QS-09-02	Hydrothermal calcite	−3.4	18.9	
QS-09-03	Hydrothermal calcite	−4.3	19.0	
QS-09-06	Hydrothermal calcite	−3.9	19.4	
QS-09-12	Hydrothermal calcite	−5.0	19.6	

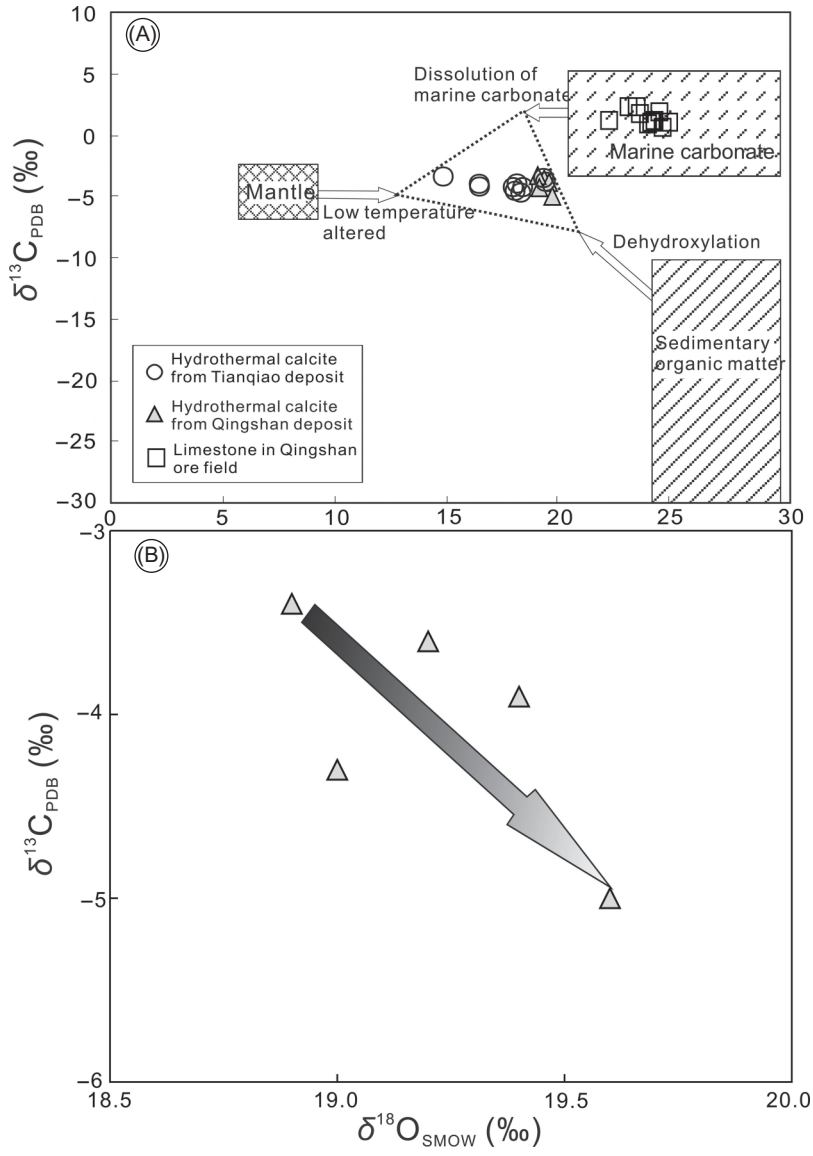

Figure 4. Plots of $\delta^{13}C_{PDB}$ *versus* $\delta^{18}O_{SMOW}$ for the Qingshan Pb–Zn deposit. C and O isotope compositions of the Tianqiao deposit are taken from Zhou *et al.* (2013).

$\delta^{13}C_{PDB}$ and $\delta^{18}O_{SMOW}$ values ranging from +0.6‰ to +2.3‰ and +22.1‰ to +24.7‰, respectively, higher than hydrothermal calcite, but similar to marine carbonate rocks.

5.2. *Sulphur isotope compositions*

S isotope compositions of sulphide minerals, together with previously published data (Zhang *et al.* 1999; Fu 2004; Gu 2007) are listed in Table 2 and shown in a histogram (Figure 5). Sulphide minerals are all enriched in heavy sulphur isotopes with $\delta^{34}S_{CDT}$ values range from +10.7‰ to +19.6‰ (Table 2; Figure 5). Pyrite, sphalerite, and galena separates have slightly different $\delta^{34}S$ values, ranging from +10.7‰ to +18.3‰, +15.7‰ to +19.6‰, and +11.4‰ to +17.2‰, respectively.

5.3. *Lead isotope compositions*

Pb isotope compositions of sulphide minerals and ores (Wang 1993; Zhang *et al.* 1999; Fu 2004) are listed in Table 3. Sulphide minerals and ores have homogeneous and low radiogenic Pb isotope compositions with $^{206}Pb/^{204}Pb$ ranging from 18.561 to 18.768, $^{207}Pb/^{204}Pb$ ranging from 15.701 to 15.920, and $^{208}Pb/^{204}Pb$ ranging from 38.831 to 39.641.

5.4. *Rb–Sr isotope compositions*

Sphalerite separates are analysed for Rb–Sr isotope (Table 4). These separates have $^{87}Rb/^{86}Sr$ ratios ranging from 0.278 to 0.846. $^{87}Sr/^{86}Sr$ ratios of sphalerite are relatively homogeneous and range from 0.7107 to 0.7141.

Table 2. Sulphur isotope compositions of ores and sulphide minerals, and sediment barite from the Qingshan Pb–Zn deposit.

Sample no.	Object	$\delta^{34}S_{CDT}$/‰	Sources
QSC-4S	Pyrite	18.3	Zhang *et al*. (1999); Gu (2007)
1800A4-S2	Sphalerite	17.6	
1816B4-S1	Sphalerite	18.5	
QSC-3S1	Sphalerite	18.4	
1816B4-S2	Galena	17.2	
1800A4-S1	Galena	15.9	
QSC-3S2	Galena	15.8	
QS03	Pyrite	16.9	Fu (2004)
QS04-1	Sphalerite	18.5	
QS04-2	Galena	14.0	
QS02	Galena	13.7	
Q-1	Sediment barite	28.3	Gu (2007)
Q-2-1	Sphalerite	15.9	
Q-2-2	Galena	11.4	
Q-6	Sphalerite	15.7	
QS01SP	Sphalerite	17.5	Zhang *et al*. (1999)
QS01	Sphalerite	16.8	
GQ3-Py	Pyrite	10.7	
F9-Py	Pyrite	12.6	
GQ11-Cc	Pyrite	13.6	
Q-Py	Pyrite	14.0	
Q-Sph	Sphalerite	19.6	
Q-Gal	Galena	16.8	
S-11	Sediment barite	23.1	
GQ0-52-2	Sediment barite	27.5	
QS-09-01	Pyrite	17.2	This article
QS-09-02	Sphalerite	16.5	
QS-09-03	Sphalerite	17.5	
QS-09-06	Sphalerite	18.2	
QS-09-12	Galena	15.5	

6. Discussion

6.1. *Possible origin of CO_2 in hydrothermal fluids*

Limestone samples from the Qingshan ore field fall in the field for marine carbonate in Figure 4A, suggesting that the wall carbonate rocks had a marine genesis, in accordance with the geological setting. Hydrothermal calcite separates are plotted in the field among mantle, marine carbonate rocks, and sedimentary organic matter, with a weakly negative correlation in the plot of $\delta^{13}C_{PDB}$ *versus* $\delta^{18}O_{SMOW}$ values (Figure 4A). If CO_2 in hydrothermal fluids derived from mantle, precipitated calcite would show constant $\delta^{13}C$ values with high $\delta^{18}O$ values (Figure 4A). Similarly, if CO_2 originated from marine carbonate, precipitated calcite would display constant $\delta^{13}C_{PDB}$ values with low $\delta^{18}O_{SMOW}$ values (Figure 4A). The negative correlation between $\delta^{13}C_{PDB}$ and $\delta^{18}O_{SMOW}$ values (Figure 4B) indicates that CO_2 in hydrothermal fluids derived from neither mantle and/or marine carbonate nor from organic matter. Because organic matter acted as a reducing agent in the thermal chemical sulphate reduction process (e.g., Ottaway *et al.* 1994; Worden *et al.* 1995), it is also an important contributor of CO_2. Therefore, a mixture of ternary members is a possible origin of CO_2. There are ^{18}O-depleted Permian Emeishan flood basalts, ^{18}O-enriched to Carboniferous to Permian carbonate rocks, and ^{13}C-depleted organic matter in host strata (Figure 4A).

6.2. *Possible sources of sulphur*

Primary ores from the Qingshan Pb–Zn deposit are composed chiefly of galena, sphalerite, and pyrite. The lack of sulphate minerals in the ores suggests that the $\delta^{34}S$ value of sulphide minerals can basically represent the $\delta^{34}S_{\sum S\text{-fluids}}$ value of hydrothermal fluids (Ohmoto 1972). All sulphide minerals have relatively enriched heavy sulphur isotopes with $\delta^{34}S$ values ranging from +11‰ to +19‰ (Figure 5A and Table 2), unlike mantle-derived sulphur (~0‰; Chaussidon *et al.* 1989). Devonian to Permian strata in the mining field contain evaporites such as gypsum and barite that have $\delta^{34}S$ values of ~+15‰ and +23‰ to +28‰, respectively (Liu and Lin 1999; Jin 2008), similar to Devonian to Permian seawater sulphate (+20‰ to +35‰; Claypool *et al.* 1980; Seal 2006). As $\Delta^{34}S_{sulphur–sulphide}$ could be up to +10‰ to +15‰ in Mississippi Valley-type Zn–Pb mineralizing systems (Ohmoto *et al.* 1990; Machel *et al.* 1995; Ohmoto and Goldhaber 1997), so the sulphur isotope signature of the

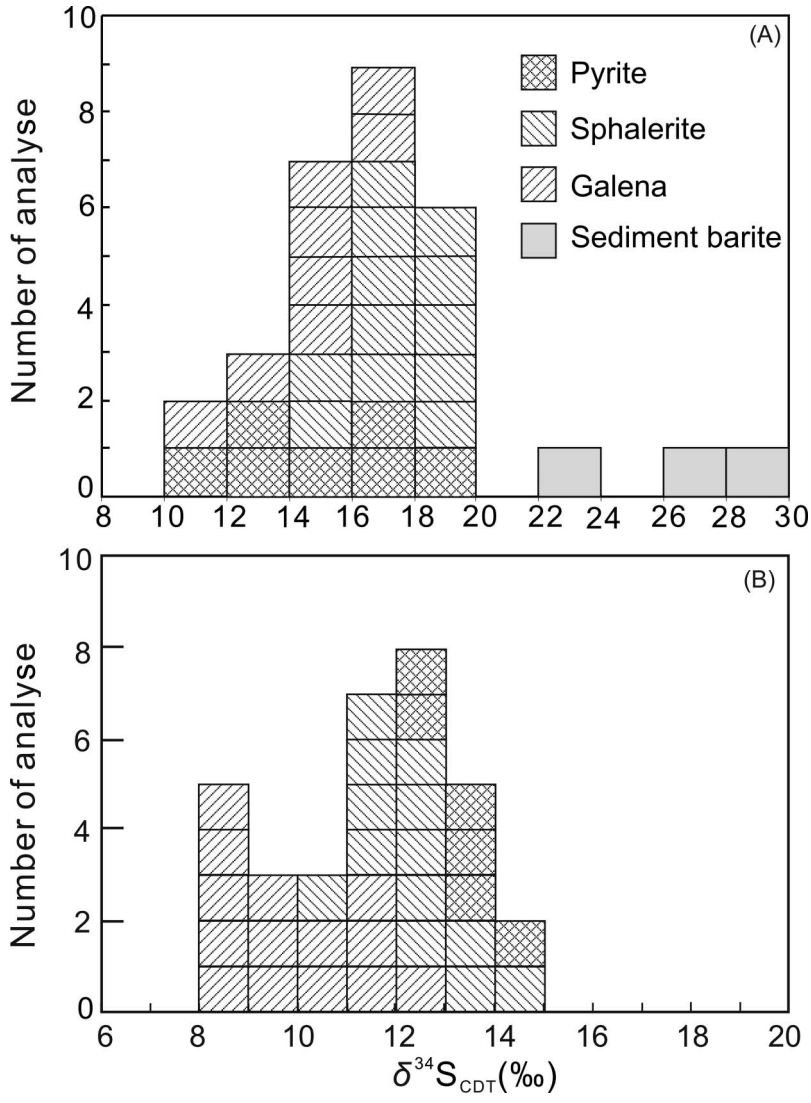

Figure 5. S isotope composition histogram of the Qingshan Pb–Zn deposit (A) and the Tianqiao Pb–Zn deposit (B). The S isotope compositions of the Tianqiao deposit are taken from Zhou *et al.* (2013).

Qingshan deposit indicates that reduced sulphur in the ores derived from evaporites in host strata (Han *et al.* 2007; Basuki *et al.* 2008). Some studies have confirmed that the reaction $SO_4^{2-} + CH_4 \rightarrow H_2S + CO_3^{2-} + H_2O$ can take place at 140°C (e.g. Worden *et al.* 1995), indicating that the thermal chemical sulphate reduction could be a way that transferred SO_4^{2-} from sulphate into H_2S in hydrothermal solutions.

6.3. Possible sources of ore-forming metals

6.3.1. Constraints of Pb isotopes

Although some studies have suggested that the metals of the Qingshan deposit were provided by Cambrian sedimentary rocks (Zhang *et al.* 1999), other studies of the SYG province have suggested that Cambrian to Permian sedimentary rocks were important sources of metals (Li *et al.* 1999). On the other hand, Jin (2008) suggested that metals were derived from Proterozoic basement rocks (such as Huili and Kunyang Groups), whereas Zhou *et al.* (2001) considered that metals were provided by Neoproterozoic volcanic rocks.

Contents of U and Th for the sulphide minerals are too low to influence the Pb isotope compositions, whereas contrasted whole rocks of basalts and sedimentary and basement rocks need to be adjusted (e.g. Carr *et al.* 1995; Zhang *et al.* 2002). Ores and sulphide minerals from the Qingshan deposit have homogeneous Pb isotope compositions (Table 3), unlike Permian Emeishan flood basalts (e.g. Huang *et al.* 2004; Yan *et al.* 2007), Sinian to Permian carbonate rocks (e.g. Zheng and Wang 1991; Zhou *et al.* 2001, 2013; Huang *et al.* 2004; Han *et al.* 2007; Jin

Table 3. Pb isotope compositions of ores and sulphide minerals from the Qingshan Pb–Zn deposit.

Sample no.	Object	$^{206}Pb/^{204}Pb$	$^{207}Pb/^{204}Pb$	$^{208}Pb/^{204}Pb$	Sources
QS04	Sphalerite	18.594	15.711	39.130	Fu (2004)
QS03	Pyrite	18.768	15.920	38.831	
QS04	Galena	18.717	15.863	39.631	
QS02	Galena	18.660	15.789	39.389	
Q3	Ores	18.667	15.802	39.480	Wang (1993)
Q5	Ores	18.591	15.701	39.166	
Qt-2	Ores	18.592	15.726	39.183	
1816A4-Pb1	Galena	18.575	15.701	39.101	Zhang *et al*. (1999)
1816B4-Pb1	Galena	18.717	15.854	39.641	
Qsc-3Pb1	Galena	18.561	15.792	39.167	
QS-09-01	Pyrite	18.619	15.816	39.121	This article
QS-09-02	Sphalerite	18.598	15.792	39.354	
QS-09-03	Sphalerite	18.652	15.780	39.455	
QS-09-06	Sphalerite	18.615	15.825	39.013	
QS-09-12	Galena	18.620	15.891	39.228	

Table 4. Rb–Sr isotope compositions of sphalerite separates from the Qingshan Pb–Zn deposit.

Samples No.	Object	Rb	Sr	$^{87}Rb/^{86}Sr$	$^{87}Sr/^{86}Sr$	$(^{87}Sr/^{86}Sr)_t$	Sources
1800A4-RS1	Sphalerite	0.368	1.255	0.846	0.7127	0.7103	Gu (1997)
1800A4-RS2	Sphalerite	0.315	2.079	0.437	0.7117	0.7105	
1800A4-RS3	Sphalerite	0.317	1.140	0.801	0.7136	0.7113	
1800A4-RS4	Sphalerite	0.344	1.528	0.659	0.7122	0.7103	
1800A4-RS5	Sphalerite	0.850	8.834	0.278	0.7107	0.7099	
QS-09-02	Sphalerite	0.336	1.612	0.312	0.7131	0.7122	This article
QS-09-03	Sphalerite	0.651	3.125	0.511	0.7141	0.7126	
QS-09-06	Sphalerite	0.518	2.156	0.425	0.7126	0.7114	

Note: $(^{87}Sr/^{86}Sr)_t = {}^{87}Sr/^{86}Sr - {}^{87}Sr/^{87}Rb\ (e^{\lambda t} - 1)$, $\lambda_{Rb} = 1.41 \times 10^{-11}\ t^{-1}$, $t = 200$ Ma.

2008), and Proterozoic basement rocks (e.g. Huang *et al.* 2004; Zhou *et al.* 2013). In the plot of $^{206}Pb/^{204}Pb$ *versus* $^{207}Pb/^{204}Pb$ (Figure 6), all samples from the Qingshan deposit fall close to the upper crust Pb evolution curve of Zartman and Doe (1981), within the field for Devonian to Permian carbonate rocks, near to basement rocks, but unlike flood basalts and Sinian Dengying Formation dolostone (Figure 6). The Qingshan Pb is slightly higher than the Tianqiao Pb (Figure 6), indicating that Pb from the Qingshan deposit is most consistent with derivation from the host carbonate rocks, whereas the Tianqiao Pb probably came from a mixed source of basement rocks and host strata (Zhou *et al.* in press).

6.3.2. Constraints of Sr isotopes

Previous studies have yielded a hydrothermal calcite Sm–Nd age (222 ± 14 Ma) of the Huize Pb–Zn deposit (Li *et al.* 2007) and sulphide Rb–Sr ages of the Paoma (200.1 ± 4.0 Ma; Lin *et al.* 2010) and Tianqiao Pb–Zn deposits (191.9 ± 6.9 Ma; Zhou *et al.* 2013). Therefore, an age of ~200 Ma is considered to be the main timing of Pb–Zn mineralization in the SYG province.

Initial $^{87}Sr/^{86}Sr_{\ 200\ Ma}$ ratios of sphalerite separates from the Qingshan deposit range from 0.7099 to 0.7126 (Table 4), higher than simultaneous Permian Emeishan flood basalts (0.7039–0.7078; Huang *et al.* 2004) and Sinian to Permian sedimentary rocks (0.7073–0.7111; Hu 1999; Deng *et al.* 2000; Zhou *et al.* 2013). However, Proterozoic basement rocks have $^{87}Sr/^{86}Sr_{\ 200\ Ma}$ ratios (0.7243–0.7288; Li and Qin 1988; Chen and Ran 1992) that are higher than the ores. Neither the older basement nor the younger cover rocks match the ore $^{87}Sr/^{86}Sr$ ratios (Figure 7), and so either there is a third source not considered in this study, or the ore strontium was sourced from a mixture of radiogenic Sr-enriched basement rocks and a radiogenic Sr-depleted cover sequence.

6.4. Implications for mineralization process

At about 200 Ma, the Yangtze Block collided with adjacent blocks associated with the closure of the Tethys Ocean (e.g. Zhang *et al.* 2006; Reid *et al.* 2007), which is known as the Indosinian Orogeny. Thermal activity related to this event resulted in hydrothermal fluids and extraction of metals from Devonian to Permian sedimentary rocks. Extensive hydrothermal fluid migration and circulation resulted in reduction of sulphur from evaporites in Cambrian to Permian sedimentary rocks. In

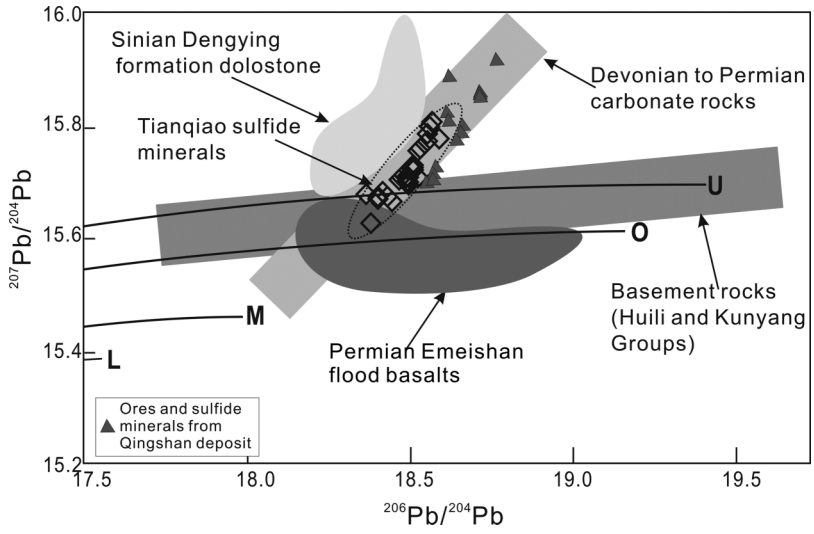

Figure 6. Plot of $^{207}Pb/^{204}Pb$ *versus* $^{206}Pb/^{204}Pb$ for the Qingshan Pb–Zn deposit. Trends for the upper crust (U), orogenic belt (O), mantle (M), and lower crust (L) are taken from Zartman and Doe (1981). Pb isotope compositions of the Tianqiao Pb–Zn deposit are from Zhou *et al.* (2013). Sources of other data are Zheng and Wang (1991), Hu (1999), Zhou *et al.* (2001, 2013), Huang *et al.* (2004), Han *et al.* (2007), and Jin (2008, this study).

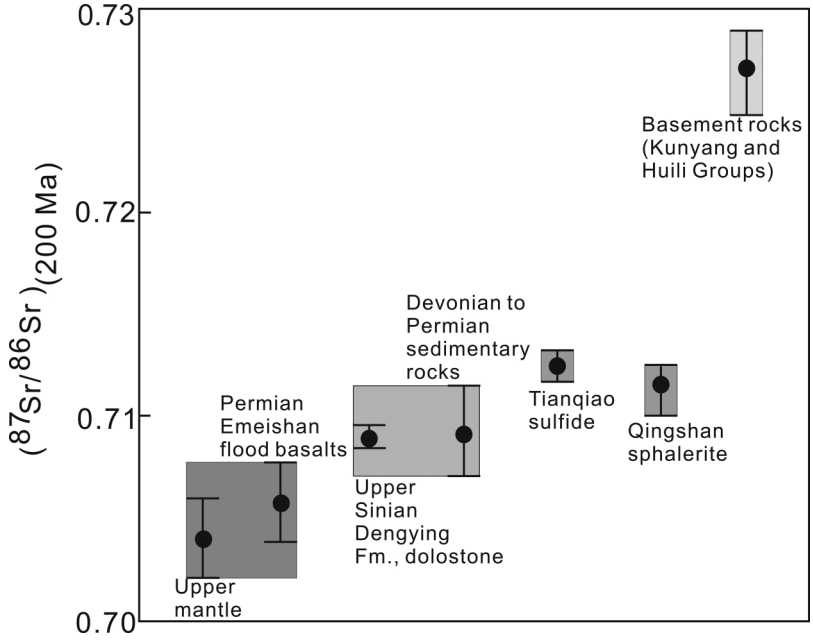

Figure 7. Comparison of $(^{87}Sr/^{86}Sr)_t$ (t= 200 Ma) ratios among the Qingshan and Tianqiao Pb–Zn deposits, Sinian to Permian sedimentary rocks, Proterozoic basement rocks, Permian Emeishan flood basalts, and upper mantle. Sr isotope compositions of the Tianqiao deposit are taken from Zhou *et al.* (2013). Sources of other data are Li and Qin (1988), Chen and Ran (1992), Zheng and Wang (1991), Gu *et al.* (1997), Hu (1999), Deng *et al.* (2000), Zhou *et al.* (2001, 2013), Huang *et al.* (2004), and Han *et al.* (2007).

addition to the Palaeozoic sedimentary rocks, the Pb–Zn enriched Proterozoic basement rocks provided metals for hydrothermal solutions. Hydrothermal fluids circulated underneath the Permian Emeishan flood basalts, whereas the basalts acted as an impermeable layer. Driven by tectonic movement and heat, the resulting ore-forming fluids enriched in Pb–Zn–Ag–Ge metals migrated upward along the Weining–Shuicheng and Yadu–Mangdong regional faults (Figure 1B), and incorporated reduced sulphur-bearing solutions, leading to the precipitation of Pb–Zn ores along folds and their intraformational faults (Figure 2).

7. Conclusions

(1) The Qingshan Pb–Zn deposit is hosted in Carboniferous-to-Permian dolomitic limestone and was structurally controlled by the Weining–Shuicheng anticline and its intraformational faults.

(2) CO_2 in the hydrothermal fluids has a mixed source of basalts, carbonate rocks, and organic matter, whereas reduced sulphur was derived from evaporites in the host strata. The Pb metal also originated from the host rocks, whereas the ore strontium had a more complex derivation involving older basement rocks and the younger cover sequence.

Acknowledgements

This research was financially supported by the National Natural Science Foundation of China (Nos. 41102055, 41272111, and 41102053). Thanks are given to Dr Jian-Feng Gao and Professor David Huston, Mei-Fu Zhou and Lin Ye for useful discussion.

References

Basuki, N.I., Taylor, B.E., and Spooner, E.T.C., 2008, Sulfur isotope evidence for thermochemical reduction of dissolved sulfate in Mississippi valley type zinc–lead mineralization, Bongara area, northern Peru: Economic Geology, v. 103, p. 183–799.

Belshaw, N.S., Freedman, P.A., O'Nions, R.K., Frank, M., and Guo, Y., 1998, A new variable dispersion double-focusing plasma mass spectrometer with performance illustrated for Pb isotopes: International Journal of Mass Spectrometry, v. 181, p. 51–58.

Carr, G.R., Dean, J.A., Suppel, D.W., and Heithersay, P.S., 1995, Precise lead isotope fingerprinting of hydrothermal activity associated with Ordovician to Carboniferous metallogenic events in the Lachlan fold belt of New South Wales: Economic Geology, v. 90, p. 1467–1505.

Chaussidon, M., Albarède, F., and Sheppard, S.M.F., 1989, Sulphur isotope variations in the mantle from ion microprobe analyses of micro-sulphide inclusions: Earth and Planetary Science Letters, v. 92, p. 144–156.

Chen, H.S., and Ran, C.Y., 1992, Isotope geochemistry of copper deposit in Kangdian area: Beijing, Geological Publishing House, p. 1–25 (in Chinese).

Chen, S.J., 1986, A discussion on the sedimentary origin of Pb–Zn deposits in western Guizhou and northeastern Yunnan: Guizhou Geology, v. 8, p. 35–39 (in Chinese with English abstract).

Chung, S.L., and Jahn, B.M., 1995, Plume–lithosphere interaction in generation of the Emeishan flood basalts at the Permian–Triassic boundary: Geology, v. 23, p. 889–892.

Claypool, G.E., Holser, W.T., Kaplan, I.R., Sakai, H., and Zak, I., 1980, The age curves of sulfur and oxygen isotopes in marine sulfate and their mutual interpretation: Chemical Geology, v. 28, p. 199–260.

Cromie, P.W., Gosse, R.R., Zhang, P., and Zhu, X., 1996, Exploration for carbonate-hosted Pb–Zn deposits, Sichuan, P.R.C.: 30th International Geological Congress, Beijing, China, Abstracts, 412 p.

Deng, H.L., Li, C.Y., Tu, G.Z., Zhou, Y.M., and Wang, C.W., 2000, Strontium isotope geochemistry of the Lemachang independent silver ore deposit, northeastern Yunnan, China: Science China Earth Science, v. 43, p. 337–346.

Dou, S., and Zhou, J.X., 2013, Geology and C-O isotope geochemistry of carbonate-hosted Pb-Zn deposits, NW Guizhou province, SW China: Chinese Journal of Geochemistry, v. 32, p. 7–18.

Friedman, I., and O'Neil, J.R., 1977, Compilation of stable isotope fractionation factors of geochemical interest: Data of Geochemistry, U.S. Geological Survey Professional Paper, p. 440–KK.

Fu, S.H., 2004, Metallogenesis of Pb-Zn deposits and enrichment regularity of dispersed elements Cd, Ga and Ge in SW Yangtze Block [Ph.D. thesis]: Chengdu University of Science and Technology, Chengdu, China, p. 20–67 (in Chinese with English abstract).

Gu, S.Y., 2007, Study on the sulfur isotope compositions of lead–zinc deposits in northwestern Guizhou Province: Journal of Guizhou University of Technology, v. 36, p. 8–13 (in Chinese with English abstract).

Gu, S.Y., Zhang, Q.H., and Mao, J.Q., 1997, The strontium isotope evidence for two solutions mixing in Qingshan lead–zinc deposit of Guizhou: Journal of Guizhou University and Technology, v. 26, p. 50–54 (in Chinese with English abstract).

Han, R.S., Hu, Y.Z., Wang, X.K., Hou, B.H., Huang, Z.L., Chen, J., Wang, F., Wu, P., Li, B., Wang, H.J., Dong, Y., and Lei, L., 2012, Mineralization model of rich Ge–Ag bearing Zn–Pb polymetallic deposit concentrated district in northeastern Yunnan, China: Acta Geologica Sinica, v. 86, p. 280–294 (in Chinese with English abstract).

Han, R.S., Liu, C.Q., Huang, Z.L., Chen, J., Ma, D.Y., Lei, L., and Ma, G.S., 2007, Geological features and origin of the Huize carbonate-hosted Zn–Pb–(Ag) District, Yunnan, South China: Ore Geology Reviews, v. 31, p. 360–383.

Han, R.S., Liu, C.Q., Huang, Z.L., Ma, D.Y., Li, Y., Hu, B., Ma, G.S., and Lei, L., 2004, Fluid inclusion of calcite and sources of ore-forming fluids in the Huize Zn–Pb–(Ag–Ge) district, Yunnan, China: Acta Geologica Sinica (English edition), v. 78, p. 583–591.

Hu, R.Z., and Zhou, M.F., 2012, Multiple Mesozoic mineralization events in South China – An introduction to the thematic issue: Mineralium Deposita, v. 47, p. 579–588.

Hu, Y.G., 1999, Ag occurrence, source of ore-forming metals and mechanism of Yinchangpo Ag–Pb–Zn deposit, Guizhou [Ph.D. thesis]: Institute of Geochemistry, Chinese Academy of Sciences, p. 10–55 (in Chinese with English abstract).

Huang, Z.L., Chen, J., Han, R.S., Li, W.B., Liu, C.Q., Zhang, Z.L., Ma, D.Y., Gao, D.R., and Yang, H.L., 2004, Geochemistry and Ore-Formation of the Huize Giant Lead–Zinc Deposit, Yunnan, Province, China: Discussion on the Relationship between the Emeishan Flood Basalts and Lead–Zinc Mineralization: Beijing, Geological Publishing House, p. 1–214 (in Chinese).

Huang, Z.L., Li, W.B., Chen, J., Han, R.S., Liu, C.Q., Xu, C., and Guan, T., 2003, Carbon and oxygen isotope constraints on the mantle fluids join the mineralization of the Huize super-large Pb–Zn deposits, Yunnan Province, China: Journal of Geochemistry Exploration, v. 78/79, p. 637–642.

Huang, Z.L., Li, X.B., Zhou, M.F., Li, W.B., and Jin, Z.G., 2010, REE and C–O isotopic geochemistry of calcites from the word-class Huize Pb–Zn deposits, Yunnan, China: Implication for the ore genesis: Acta Geologica Sinica (English edition), v. 84, p. 597–613.

Huston, D.L., Sie, S.H., Suter, G.F., Cooke, D.R., and Both, R.A., 1995, Trace elements in sulfide minerals from Eastern Australian volcanic-hosted massive sulfide deposits: Part

1. Proton microprobe analyses of pyrite, chalcopyrite, and sphalerite, and Part 2. Selenium levels in pyrite: Comparison with $\delta^{34}S$ values and implications for the source of sulfur in volcanogenic hydrothermal systems: Economic Geology, v. 90, p. 1167–1196.

Jin, Z.G., 2008, The Ore-control factors, ore-forming regularity and forecasting of Pb–Zn deposit, in Northwestern Guizhou Province: Beijing, Engine Industry Press, p. 1–105 (in Chinese).

Leach, D.L., Bradley, D.C., Huston, D., Pisarevsky, S.A., Taylor, R.D., and Gardoll, S.J., 2010, Sediment-hosted lead–zinc deposits in Earth history: Economic Geology, v. 105, p. 593–625.

Li, F.H., and Qin, J.M., 1988, Presinian system in Kangdian area: Chongqing, Chongqing Press, p. 15–45 (in Chinese).

Li, L.J., Liu, H.T., and Liu, J.S., 1999, A discussion on the source bed of Pb–Zn–Ag deposits in northeast Yunnan: Geological Exploration for Non-Ferrous Metals, v. 8, p. 333–339 (in Chinese with English abstract).

Li, Q.L., Chen, F.K., Wang, X.L., and Li, C.F., 2005, Ultra-low procedural blank and the single grain mica Rb-Sr isochron dating: Chinese Science Bulletin, v. 50, p. 2861–2865.

Li, W.B., Huang, Z.L., and Yin, M.D., 2007, Dating of the giant Huize Zn–Pb ore field of Yunnan province, Southwest China: Constraints from the Sm–Nd system in hydrothermal calcite: Resource Geology, v. 57, p. 90–97.

Liao, W., 1984, A discussion on the S and Pb isotopic composition characteristics and metallogenic model of the Pb–Zn ore zones in eastern Yunnan and western Guizhou: Journal of Geology and Exploration, v. 1, p. 1–6 (in Chinese with English abstract).

Lin, Z.Y., Wang, D.H., and Zhang, C.Q., 2010, Rb-Sr isotopic age of sphalerite from the Paoma lead-zinc deposit in Sichuan Province and its implications: Geology in China, v. 37, p. 488–196 (in Chinese with English abstract).

Liu, H.C., and Lin, W.D., 1999, Study on the law of Pb–Zn–Ag ore deposit in Northeast Yunnan, China: Kunming, Yunnan University Press, p. 1–468 (in Chinese).

Machel, H.G., Krouse, H.R., and Sassen, R., 1995, Products and distinguishing criteria of bacterial and thermochemical sulfate reduction: Applied Geochemistry, v. 10, p. 373–389.

Mao, J.Q., Zhang, Q.H., and Gu, S.Y., 1998, Tectonic evolution and Pb–Zn mineralization of Shuicheng fault subsidence: Guiyang, Guizhou Science and Technology Publishing Company, p. 104–129 (in Chinese).

Ohmoto, H., 1972, Systematics of sulfur and carbon isotopes in hydrothermal ore deposits: Economic Geology, v. 67, p. 551–579.

Ohmoto, H., and Goldhaber, M.B., 1997, Sulfur and carbon isotopes, *in* Barnes, H.L., ed., Geochemistry of Hydrothermal Ore Deposits (third edition): New York, Wiley, p. 517–611.

Ohmoto, H., Kaiser, C.J., and Geer, K.A., 1990, Systematics of sulphur isotopes in recent marine sediments and ancient sediment-hosted base metal deposits, *in* Herbert, H.K., and Ho, S.E., eds., Stable isotopes and fluid processes in mineralisation: Australia, University of Western Australia, v. 23, p. 70–120.

Ottaway, T.L., Wicks, F.J., and Bryndzia, L.T., 1994, Formation of the Muzo hydrothermal deposit in Colombia: Nature, v. 369, p. 552–554.

Reid, A., Wilson, C.J.L., Shun, L., Pearson, N., and Belousova, E., 2007, Mesozoic plutons of the Yidun Arc, SW China: U/Pb geochronology and Hf isotopic signature: Ore Geology Reviews, v. 31, p. 88–106.

Seal, I.R., 2006, Sulfur isotope geochemistry of sulfide minerals: Review of Mineralogy and Geochemistry, v. 61, p. 633–677.

Sun, W.H., Zhou, M.F., Gao, G.F., Yang, Y.H., Zhao, X.F., and Zhao, J.H., 2009, Detrital zircon U–Pb geochronological and Lu–Hf isotopic constraints on Detrital zircon U–Pb geochronological and Lu–Hf isotopic constraints on the Precambrian magmatic and crustal evolution of the western Yangtze Block, SW China: Precambrian Research, v. 172, p. 99–126.

Tu, G.Z., 1984, Geochemistry of strata-bound ore deposits in China (Volume I): Beijing, Science Press, p. 13–69 (in Chinese with English abstract).

Wang, C.M., Deng, J., Zhang, S.T., Xue, C.J., Yang, L.Q., Wang, Q.F., and Sun, X., 2010, Sediment-hosted Pb–Zn deposits in southwest Sanjiang Tethys and Kangdian area on the western margin of Yangtze Craton: Acta Geologica Sinica (English Edition), v. 84, p. 1428–1438.

Wang, H.Y., 1993, Geochemistry of Pb–Zn mineralization in Guizhou: Guizhou Geology, v. 10, p. 272–290 (in Chinese with English abstract).

Wang, J.Z., Li, Z.Q., and Ni, S.J., 2003, Origin of ore-forming fluids of Mississippi Valley-type (MVT) Pb–Zn deposits in Kangdian area, China: Chinese Journal of Geochemistry, v. 22, p. 369–376.

Wang, X.C., Zheng, Z.R., Zheng, M.H., and Xu, X.H., 2000, Metallogenic mechanism of the Tianbaoshan Pb–Zn deposit, Sichuan: Chinese Journal of Geochemistry, v. 19, p. 121–133.

Wilkinson, J.J., Eyre, S.L., and Boyce, A.J., 2005, Ore-forming processes in Irish-type carbonate-hosted Zn–Pb deposits: Evidence from mineralogy, chemistry, and isotopic composition of sulfides at the Lisheen Mine: Economic Geology, v. 100, p. 63–86.

Worden, R.H., Smalley, P.C., and Oxtoby, N.H., 1995, Gas souring by the thermo chemical sulfate reduction at 140°C: AAPG Bulletin, v. 79, p. 854–863.

Xie, J.R., 1963, Introduction of the Chinese ore deposits: Beijing, Science Publishing House, p. 1–71 (in Chinese).

Yan, D.P., Zhou, M.F., Song, H.L., Wang, X.W., and Malpas, J., 2003, Origin and tectonic significance of a Mesozoic multi-layer over-thrust system within the Yangtze Block (South China): Tectonophysics, v. 361, p. 239–254.

Yan, Z.F., Huang, Z.L., Xu, C., Chen, M., and Zhang, Z.L., 2007, Signatures of the source for the Emeishan flood basalts in the Ertan area: Pb isotope evidence: Chinese Journal of Geochemistry, v. 26, p. 207–213.

Yavuz, F., Jiang, S.Y., Karakaya, N., Karakaya, M.C., and Yavuz, R., 2011, Trace element, rare-earth elements and boron isotopic compositions of tourmaline from a vein-type Pb–Zn–Cu ± U deposit, NE Turkey: International Geology Review, v. 53, p. 1–24.

Zartman, R.E., and Doe, B.R., 1981, Plumbotectonics – The model: Tectonophysics, v. 75, p. 135–162.

Zhang, Q., Liu, J.J., and Shao, S.X., 2002, An estimate of the lead isotopic compositions of upper mantle and upper crust and implications for the source of lead in the Jinding Pb–Zn deposit in western Yunnan, China: Geochemical Journal, v. 36, p. 271–287.

Zhang, Q.H., Guang, S.Y., and Mao, J.Q., 1999, Geochemical study on Qingshan lead–zinc deposit in Shuicheng, Guizhou province: Geology–Geochemistry, v. 27, p. 15–20 (in Chinese with English abstract).

Zhang, Z.B., Li, C.Y., Tu, G.C., Xia, B., and Wei, Z.Q., 2006, Geotectonic evolution background and ore-forming process of Pb-Zn deposits in Chuan–Dian–Qian area of Southwest China: Geotectonica et Metallogenia, v. 30, p. 343–354 (in Chinese with English abstract).

Zhao, X.F., Zhou, M.F., Li, J.W., Sun, M., Gao, J.F., Sun, W.H., and Yang, J.H., 2010, Late Paleoproterozoic to early

Mesoproterozoic Dongchuan Group in Yunnan, SW China: Implications for tectonic evolution of the Yangtze Block: Precambrian Research, v. 182, p. 57–69.

Zheng, C.L., 1994, An approach on the source of ore-forming metals of lead–zinc deposits in Northwestern part, Guizhou, Province: Journal of Guilin College of Geology, v. 14, p. 113–124 (in Chinese with English abstract).

Zheng, M.H., and Wang, X.C., 1991, Genesis of the Daliangzi Pb–Zn deposit in Sichuan, China: Economic Geology, v. 86, p. 831–846.

Zhou, C.X., Wei, C.S., and Guo, J.Y., 2001, The source of metals in the Qilingchang Pb–Zn deposit, Northeastern Yunnan, China: Pb–Sr isotope constraints: Economic Geology, v. 96, p. 583–598.

Zhou, J.X., Huang, Z.L., Zhou, G.F., Li, X.B., Ding, W., and Bao, G.P., 2010, Sulfur isotopic compositions of the Tianqiao Pb–Zn ore deposit, Guizhou Province, China: Implications for the source of sulfur in the ore-forming fluids: Chinese Journal of Geochemistry, v. 29, p. 301–306.

Zhou, J.X., Huang, Z.L., Zhou, G.F., Li, X.B., Ding, W., and Bao, G.P., 2011, Trace elements and rare earth elements of sulfide minerals in the Tianqiao Pb–Zn Ore deposit, Guizhou province, China: Acta Geologica Sinica (English edition), v. 85, p. 189–199.

Zhou, J.X., Huang, Z.L., Zhou, M.F., Li, X.B., and Jin, Z.G., 2013, Constraints of C–O–S–Pb isotope compositions and Rb–Sr isotopic age on the origin of the Tianqiao carbonate-hosted Pb–Zn deposit, SW China: Ore Geology Reviews, doi:10.1016/j.oregeorev.2013.01.001.

Zhou, M.F., Yan, D.P., Kennedy, A.K., Li, Y.Q., and Ding, J., 2002, SHRIMP zircon geochronological and geochemical evidence for Neo-proterozoic arc-related magmatism along the western margin of the Yangtze Block, South China: Earth and Planetary Science Letters, v. 196, p. 1–67.